南京航空航天大学

论文集

（二〇〇九年） 第4册

航空宇航学院

（第4分册）

南京航空航天大学科技部编

二〇一〇年五月

航空宇航学院

013

航空宇航学院2009年学术论文清单（0134）

序号	姓名	职称	单位	论文题目	刊物、会议名称	年、卷、期
1	裘进浩 姜皓 季宏丽 朱孔军	教授 硕士 博士 教授	0134 0134 0134 0134	A comparison between four piezoelectric energy harvesting circuits	Frontiers of Mechanical Engineering in China	2009. 04. 02
2	裘进浩 季宏丽 沈辉	教授 博士 博士	0134 0134 0134	Energy Harvesting and Vibration Control Using Piezoelectric Elements and a Nonlinear Approach	12th International Meeting on Ferroelectricity and 18th IEEE International Symposium on Applications of Ferroelectrics	
3	裘进浩 朱孔军 季宏丽	教授 教授 博士	0134 0134 0134	Fabrication and performance of high temperature style functionally graded piezoelectric bending actuators	Modern Physics Letters B	2009. 23. 09
4	裘进浩 季宏丽 朱孔军	教授 博士 教授	0134 0134 0134	Semi-active vibration control using piezoelectric actuators in smart structures	Front. Mech. Eng. China	2009. 04. 03
5	裘进浩 姜皓 季宏丽 朱孔军 李勇君	教授 硕士 博士 教授 硕士	0134 0134 0134 0134 0134	功能梯度压电驱动器的结构设计、制备与功能验证	光学精密工程	2009. 17. 01
6	裘进浩 边义祥 季宏丽 朱孔军	教授 博士 博士 教授	0134 0134 0134 0134	智能材料结构在航空领域中的应用	航空制造技术	2009. 03
7	季宏丽 裘进浩 朱孔军 Kazuya Matsuta	博士 教授 教授 教授	0134 0134 0134 外单位	An improved system of active noise isolation using a self-sensing actuator and neural network	Journal of Vibration and Control	2009. 15. 12
8	季宏丽 裘进浩 陈军	博士 教授 硕士	0134 0134 0134	Application of a Negative Capacitance Circuit in Synchronized Switch Damping Techniques for Vibration Suppression	The Sixth International Conference on Flow Dynamics	
9	季宏丽 裘进浩 朱孔军 陈远晟 Adrien Badel	博士 教授 教授 博士 副教授	0134 0134 0134 外单位	Multimodal vibration control using a synchronized switch based on a displacement switching threshold	Smart Materials and Structures	2009. 18. 03
10	季宏丽 裘进浩 Adrien Badel 陈远晟	博士 教授 教授 博士生	0134 0134 外单位 0134	Semi-active vibration control of a composite beam by adaptive synchronized switching on voltage sources based on LMS algorithm	Journal of Intelligent Material Systems and Structures	2009. 20. 08
11	季宏丽 裘进浩 Adrien Badel 朱孔军	博士 教授 副教授 教授	0134 0134 外单位 0134	Semi-active Vibration Control of a Composite Beam Using Adaptive SSDV Approach	Journal of Intelligent Material Systems and Structures	2009. 20. 03
12	季宏丽 裘进浩 朱孔军	博士 教授 教授	0134 0134 0134	Vibration Control of A Composite Beam by an Adaptive Semi-active Method based on LMS Algorithm	第三届全国压电与声波理论及器件技术研讨会	
13	季宏丽 裘进浩 赵永春 朱孔军	博士 教授 硕士 教授	0134 0134 0134 0134	基于TMS320F2812的悬臂梁振动半主动控制	光学精密工程	2009. 17. 1
14	边义祥 裘进浩 王鑫伟 季宏丽 朱孔军	博士 教授 教授 博士 教授	0134 0134 0132 0134 0134	The constitutive equations of half coated metal core piezoelectric fiber	International Journal of Applied Electromagnetics and Mechanics	2009. 29. 01

15	边义祥 裘进浩 王鑫伟 季宏丽 朱孔军	博士 教授 教授 博士 教授	0134 0134 0132 0134 0134	半电极含金属芯压电纤维的驱动性能	光学精密工程	2009. 17. 01
16	边义祥 裘进浩 王鑫伟 季宏丽 朱孔军	博士 教授 教授 博士 教授	0134 0134 0132 0134 0134	含金属芯压电纤维振动传感器	第三届全国压电与声波理论及器件技术研讨会	
17	阚君武 裘进浩	教授 教授	外单位 0134	Modeling and simulation of piezoelectric composite diaphragms for energy harvesting	International Journal of Applied Electromagnetics and Mechanics	2009. 30. 1-2
18	李生权 裘进浩 季宏丽 朱孔军	博士 教授 博士 教授	0134 0134 0134 0134	一类非线性非最小相位系统的神经网络逆控制	系统仿真学报	2009. 21. 04
19	刘 建 裘进浩 常伟杰 边义祥 朱孔军	博士 教授 硕士 博士 教授	0134 0134 0134 0134 0134	Research on the Response of Piezoelectric Ceramic Fibers With Metal Core to Lamb Waves	第三届全国压电与声波理论及器件技术研讨会	
20	刘 建 裘进浩 常伟杰 季宏丽 朱孔军	博士 教授 硕士 博士 教授	0134 0134 0134 0134 0134	Lamb Wave Generation and Sensing with Metal-core Piezoelectric Fibers for Structural Health Monitoring	Sixth International Conference on Flow Dynamics	
21	沈 辉 季宏丽 裘进浩 朱孔军	博士 博士 教授 教授	0134 0134 0134 0134	A Semi-passive Vibration Damping System Powered by Harvested Energy	International Journal of Applied Electromagnetics and Mechanics	2009. 31. 04
22	赵永春 季宏丽 裘进浩 朱孔军	硕士 博士 教授 教授	0134 0134 0134 0134	基于压电元件的悬臂梁半主动振动控制研究	振动、测试与诊断	2009. 29. 4
23	袁慎芳 邱雷 吴键 孙亚杰 王强	教授 博士 博士 博士 博士	0134 0134 0134 0134 0134	大型飞机的发展对结构健康监测的需求与挑战	航空制造技术	2009. 22
24	袁慎芳 邱雷 王强 苗苗 余振华	教授 博士 博士 硕士 硕士	0134 0134 0134 0134 0134	压电-光纤综合结构健康监测系统的研究及验证	航空学报	2009. 30. 02
25	吴键 袁慎芳 周根源 季赛 王子龙 王洋	博士 教授 访问学者 博士 学士 硕士	0134 0134 外单位 0134 0134 0134	Design and Evaluation of a Wireless Sensor Network Based Aircraft Strength Testing System	sensors	2009. 09. 06
26	吴键 袁慎芳 尚盈 王子龙	博士 教授 硕士 学士	0134 0134 0134 0134	Strain distribution monitoring wireless sensor network design and its evaluation research on aircraft wingbox	International Journal of Applied Electromagnetics and Mechanics	2009. 31. 01
27	吴键 袁慎芳 王子龙 王洋	博士 教授 学士 王洋	南京航空航天大学	Wireless Sensor Network Design and Performance Validation for Measurements in aircraft Strength Ground Testing	International Conference on Smart Structures and Materials (SMART' 09)	
28	孙亚杰 袁慎芳 邱雷 蔡建 王强	博士 教授 博士 博士 博士	南京航空航天大学	基于Lamb 波相控阵和图像增强方法的损伤监测	航空学报	2009. 30. 07

29	苏永振 袁慎芳 周恒芳	博士 教授 硕士	南京航空航天大学	基于三角测量和最优化技术的复合材料冲击定位两步法	宇航学报	2009.30.03
30	苏永振 袁慎芳 张炳良	博士 教授 硕士	南京航空航天大学	基于声发射和神经网络的复合材料冲击定位	传感器与微系统	2009.28.09
31	苏永振 袁慎芳	博士 教授	南京航空航天大学	基于独立分量分析的多源冲击定位方法	振动与冲击	2009.28.08
32	黄红梅 袁慎芳	博士 教授	南京航空航天大学	基于**FBG**光谱特性的修补结构中裂纹扩展的研究	光电子·激光	2009.20.10
33	黄红梅 袁慎芳	博士 教授	南京航空航天大学	基于光纤**Bragg** 光栅传感器的疲劳裂纹扩展的研究	光电子·激光	第20卷第4期
34	陈拥军 袁慎芳 王洋 吴键	博士 教授 硕士 博士	南京航空航天大学	Artificial Immune system based approach to fault diagnosis for wireless sensor networks	Second International Conference on Smart Materials and Nanotechnology in Engineering	2009.7493
35	蔡建 袁慎芳 邱雷	博士 教授 博士	南京航空航天大学	基于波包能量的裂纹扩展监测实验研究	东南大学学报(自然科学版)	2009.39.03
36	张逍越 袁慎芳 郝桐	博士 教授 学士	南京航空航天大学	Lamb wave propagation modeling for structure health monitoring	Frontiers of Mechanical Engineering in China	2009.04.03
37	张逍越 袁慎芳 邱雷	博士 教授 博士	南京航空航天大学	飞行器板结构中Lamb波解析建模研究	全国博士学术会议先进飞行器结构设计理论与技术论文集	
38	邱雷 袁慎芳 王强 孙亚杰 杨伟伟	博士 教授 博士 博士 硕士	南京航空航天大学	Design and Experiment of PZT Network-based Structural Health Monitoring Scanning System	Chinese Journal of Aeronautics	2009.22
39	邱雷 袁慎芳	博士 教授	南京航空航天大学	On development of a multi-channel PZT array scanning system and its evaluating application on UAV wing box	Sensors and Actuators A: Physical	2009.A151(2)
40	邱雷 袁慎芳 王强	博士 教授 博士	南京航空航天大学	On development of PZT array based structural health monitoringscanning system and its experimental research on UAV wing box	International Conference on Smart Structures and Materials (SMART'09)	
41	邱雷 袁慎芳 苗苗	博士 教授 硕士	南京航空航天大学	基于FBG的机翼盒段结构健康监测系统功能验证研究	压电与声光	2009.31.03
42	邱雷 袁慎芳 王强	博士 教授 博士	南京航空航天大学	基于Lamb 波主动结构健康监测系统的研制	压电与声光	2009.31.05
43	邱雷 袁慎芳	博士 教授	南京航空航天大学	一种复合材料结构损伤监测的信号合成成像方法	第十一届全国无损检测新技术交流会论文集	
44	张炳良 袁慎芳 苏永振 周恒保	硕士 教授 博士 硕士	南京航空航天大学	复合材料结构冲击定位集成监测系统的研制	2009航空试验测试技术学术交流会论文集	2009.28.增刊
45	张炳良 袁慎芳 苏永振 周恒保	硕士 教授 博士 硕士	南京航空航天大学	一种复合材料结构冲击定位集成监测系统	2009江苏省仪器仪表学会学术年会论文集	
46	王强 袁慎芳	博士 教授	南京航空航天大学	Baseline-Free Damage Imaging Method for Lamb Wave Based Structural Health Monitoring	International Conference on Smart Structures and Materials (SMART'09)	
47	王强 袁慎芳	博士 教授	南京航空航天大学	Baseline-free imaging method based on new pzt sensor arrangements	Journal of Intelligent Material Systems and Structures	2009.20.14
48	王强 袁慎芳	博士 教授	南京航空航天大学	复合材料板脱层损伤的时间反转成像监测	复合材料学报	2009.26.03

49	王强 袁慎芳	博士 教授	南京航空航天大学	主动Lamb 波损伤成像监测中的波包重建方法	宇 航 学 报	2009.30.03
50	赵霞 袁慎芳 周恒保	博士 教授 硕士	南京航空航天大学	An evaluation on the multi-agent system based structural health monitoring for large scale structure	Elsevier: Expert Systems with Applications	2009.36.03
51	尚盈 袁慎芳 吴键	硕士 教授 博士	南京航空航天大学	基于无线传感网络的大型结构健康监测系统	数据采集与处理	2009.24.02
52	常琦 袁慎芳 周恒保	博士 教授 硕士	南京航空航天大学	A design strategy of Structual health management system	14th International Symposium on Applied Electromagnetics and Mechanics	
53	常琦 袁慎芳 苗苗 王长坤	博士 教授 硕士 硕士	南京航空航天大学	基于布拉格光纤光栅的碳纤维壁板损伤监测研究	中国机械工程	2009.20.01
54	常琦 袁慎芳	博士 教授	南京航空航天大学	飞行器综合健康管理(IVHM) 系统技术现状及发展	系统工程与电子技术	2009.31.11
55	常琦 袁慎芳 周恒保	博士 教授 硕士	南京航空航天大学	基于LS-SVMs 机翼盒段壁板损伤辨识研究	压电与声光	2009.31.04
56	常琦 袁慎芳	博士 教授	南京航空航天大学	碳纤维机翼盒断壁板损伤监测研究	第十一届全国无损检测新技术交流会论文集	
57	季赛 袁慎芳 吴键	博士 教授 博士	南京航空航天大学	Using Self-organizing Map in Backbone Formation for Wireless Sensor Networks	Fifth International Conference on Natural Computaion	
58	季赛 袁慎芳 吴键	博士 教授 博士	南京航空航天大学	基于时空特性的无线传感器网络节点故障诊断方法	传感器与微系统	2009.28.10
59	胡兴柳 梁大开 芦观	博士 教授	0134 0134 0134	基于光纤智能夹层和模糊RBF神经网络的飞行器载荷识别	南京航空航天大学学报	2009.41.04
60	胡耀明 梁大开 张伟 王健	硕士 教授	0134 0134 0134 0134	基于强度调制的光纤SPR系统的研究	压电与声光	2009.31.01
61	陆观 梁大开 胡兴柳	博士 教授	0134 0134 0134	光纤智能结构的传感网络敏感区域探测	南京航空航天大学学报	2009.41.04
62	潘晓文 梁大开 芦吉云	博士 教授	0134 0134 0134	板结构试件多载荷识别算法及在损伤检测上的应用	计量学报	2009.30.02
63	张晓丽 梁大开 芦吉云 朱珠	博士 教授	0134 0134 0134 0134	多片压电双晶片并联驱动器的设计	南京航空航天大学学报	2009.41.03
64	张晓丽 梁大开 朱珠 周伟	硕士 教授	0134 0134 0134 0134	压电双晶片两种电气连接方式的实验研究	压电与声光	2009.31.05
65	周兵 梁大开 王彦	硕士 教授	0134 0134 0134	基于长周期光纤光栅的动态检测技术研究	压电与声光	2009.31.01
66	朱孔军 柳泽河 道 恩田步 武 唯芳浩 二 季宏丽 裘进浩	教授 博士 教授	0134 外单位 外单位 外单位 0134 0134	Ca-Pb-HA 固溶体的水热合成与结构表征	硅酸盐学报	2009.37.03

67	朱孔军 裘进浩	教授 教授	0134 0134	Effect of washing of barium titanate powders synthesized by hydrothermal method on their sinterability and piezoelectric propertie	Ceramics International	2009.35
68	朱孔军 裘进浩 季宏丽 Atsushi Totsuka b	教授 教授 博士	0134 0134 0134 外单位	Fabrication of lead-free barium titanate piezoelectric ceramics from barium titanate powders with different particle sizes synthesized by hydrothermal method	International Journal of Applied Electromagnetics and Mechanics	2009.31
69	朱孔军 裘进浩	教授 教授	0134	Hydrothermal synthesis of KxNa1-xNbO3 powder for fabrication of lead-free piezoelectric ceramics	Proceedings of the World Forum on Smart Materials and Smart Structures Technology	2008
70	朱孔军 孟兆磊 裘进浩 王道利 赵淳生	教授 硕士 教授 硕士 院士	0134 0134 0134 0134 0135	K0.5Na0.5NbO3无铅压电陶瓷的烧结特性	光学精密工程	2009.17.01
71	朱孔军 Kazumichi Yanagisawab Ayumu Onda Kaoji Kajiyoshi 裘进浩	教授 教授	0134 外单位 外单位 外单位 0134	Morphology variation of cadmium hydroxyapatite synthesized by high temperature mixing method under hydrothermal conditions	Materials Chemistry and Physics	2009.113
72	朱孔军 苏礼奎 季宏丽 裘进浩	教授 硕士 博士 教授	0134 0134 0134 0134	New method for fabrication of Lead-free BaTiO3 piezoelectric ceramics	PROCEEDINGS OF THE 2008 SYMPOSIUM ON PIEZOELECTRICITY, ACOUSTIC WAVES AND DEVICE APPLICATIONS	2008年
73	朱孔军 裘进浩	教授 教授	0134 0134	Synthesis and crystallographic study of Pb-Sr hydroxyapatite solid solutions by high temperature mixing method under hydrothermal conditions	Materials Research Bulletin	2009.44
74	柏林 朱孔军 裘进浩 季宏丽 苏礼奎	硕士 教授 教授 博士 硕士	0134 0134 0134 0134 0134	Phase evolution of (K,Na)NbO3 powder by high temperature mixing method under hydrothermal conditions	第六届海峡两岸超微颗粒学术研讨会	2009
75	柏林 朱孔军 苏礼奎 裘进浩 季宏丽	硕士 教授 硕士 教授 博士	0134 0134 0134 0134 0134	Synthesis of (K, Na)NbO3 particles by high temperature mixing method under hydrothermal conditions	Materials Letters	2009.64
76	刘培新 朱孔军 胡秀兰 裘进浩 纪士东	硕士 教授	0134 0134 0134 0134 0134	聚合物前躯体法制备铌酸钾钠薄膜	电子元件与材料	2009.28.09
77	罗俊 朱孔军 裘进浩 王会 季宏丽	硕士 教授 教授 硕士 博士	0134 0134 0134 0134 0134	高性能PNN-PZT压电陶瓷的制备及性能测试	2009海峡两岸功能材料论坛交流	2009
78	孟兆磊 朱孔军 裘进浩 季宏丽 吴华德	硕士 教授 教授 博士	0135 0134 0134 0134 0134	铌酸钾钠无铅压电陶瓷性能的研究	压电与声光	2009.31.03

79	苏礼奎 朱孔军 裘进浩 柏林 季宏丽	硕士 教授 教授 硕士 博士	0134 0134 0134 0134 0134	水热法合成铌酸钾钠基无铅压电陶瓷粉体的研究	2009海峡两岸功能材料论坛交流	2009年
80	苏礼奎 朱孔军 裘进浩 柏林 王会 季宏丽	硕士 教授 教授 硕士 硕士 博士	0134 0134 0134 0134 0134 0134	水热法制备(K, Na) (Nb, Sb)03粉体晶体结构及围观形貌的研究	第六届海峡两岸超微颗粒学术研讨会	2009年
81	王道利 朱孔军 裘进浩 季宏丽	硕士 教授 教授 博士	0134 013 0134 0134	Two-Step Sintering of the Pure K0.5Na0.5Nb03 Lead-Free Piezoceramiacs and Its Piezoelectric Properties	Ferroelectrics	2009.392
82	王会 朱孔军 裘进浩 罗俊 季宏丽	硕士 教授 教授 硕士 博士	0134 0134 0134 外单位 0134	流延法制备Pb(Ni1/3Nb2/3)0.5(Ti0.7Zr0.3)0.503压电陶瓷及其性能研究	2009海峡两岸功能材料论坛交流	2009
83	朱仁强 朱孔军 裘进浩 季宏丽	硕士 教授 教授 博士	0134 0134 0134 0134	共沉淀辅助水热合成球壳结构的PLZT纳米颗粒	第六届海峡两岸超微颗粒学术研讨会	2009
84	郑世杰 代锋 冯岩	教授 硕士生 硕士生	0134 0134 0134	Active control of piezothermoelastic FGM shells using integrated piezoelectric sensor/actuator layers	International Journal of Applied Electromagnetics and Mechanics	2009.3
85	郑世杰 冯岩 代锋	教授 硕士 硕士	0134 0134 0134	The simulation of active control of the shape and vibration of piezoelectric, Magneto-electro-elastic and FGM structures	Proceedings of the 2008 symposium on piezoelectricity, acoustic waves and device applications.	
86	郑世杰 李正强 王宏涛	教授 硕士生 副教授	0134 0134 0134	Research on Delamination Monitoring for Composite Structures Based on HHGA—WNN	Applied Soft Computing	2009.09.03
87	郑世杰 郭腾飞 董会丽 宋振	教授 硕士生 硕士生 硕士生	0134 0134 0134 0134	基于混合编码遗传算法和有限元分析的压电结构载荷识别	计算力学学报	2009.26.03
88	张荣祥 郑世杰 夏彦君	硕士生 教授 硕士生	0134 0134 0134	基于混沌遗传算法的布拉格光栅非均匀应变分布重构	光电子•激光	2009.20.08
89	沈星	教授	0134	Free standing Pt-Au bimetallic membranes with a leaf-like nanostructure from agarose-mediated electrodeposition and oxygen gas sensing in room temperature ionic liquids	Journal of Materials Chemistry	2009.19.41
90	沈星 刘永刚 章建文	教授 博士 硕士	0134 0134 0134	Study of Piezoelectric Fiber Composite Actuators Applied in the Flapping Wing	IEEE International Symposium on Applications of Ferroelectrics	
91	龚立娇 沈星	硕士 教授	0134 0134	Experimental Investigation of Energy Harvesting from Triple-layer Piezoelectric Bender	IEEE International Symposium on Applications of Ferroelectrics	
92	李允 沈星 王宁	硕士 教授 硕士	0134 0134 0134	1-3型压电纤维复合材料结构参数对驱动性能的影响	材料导报	2008.22.12
93	苟欢敏 徐志伟	硕士 教授	0134 0134	复合材料格栅结构的力学性能研究	兵器材料科学与工程	2009.32.06
94	安逸 熊克 顾娜	博士 教授 博士	0134 0134 0134	一种离子聚合物金属复合材料拉伸试验研究	航空学报	2009.30.05

95	安逸 熊克 顾娜	博士 教授 博士	0134 0134 0134	离子聚合物金属复合材料的力电耦合模型	材料研究学报	2009.23.04
96	安逸 熊克 顾娜	博士 教授 博士	0134 0134 0134	采用梯度功能方法的IPMC弹性模量改进模型	复合材料学报	2009.26.06
97	陈骐 熊克 卞侃 金宁 王帮峰	硕士 教授 硕士 硕士 教授	0134 0134 0134 0134 0134	Ag型IPMC柔性驱动器的制备及性能	材料科学与工程学报,	2009.27.03
98	陈骐 熊克 卞侃 金宁 王帮峰	硕士 教授 硕士 硕士 教授	0134 0134 0134 0134 0134	一种新型柔性驱动器的制备和性能研究	兵器材料科学与工程	2009.32.02
99	刘宏月 曾捷 梁大开 王晓刚	硕士 讲师 教授 硕士	0134 0134 0134 0134	基于盒膜结构的微弯式长周期光纤光栅气压传感器研究	仪器仪表学报	2009.30.08
100	潘晓文 曾捷 梁大开	博士 讲师 教授	0134 0134 0134	板结构静载荷的损伤检测算法	计量学报	2009.30.06
101	潘晓文 曾捷 梁大开	博士 讲师 教授	0134 0134 0134	光纤Bragg光栅损伤检测系统	传感器与微系统	2009.28.06
102	曾捷 梁大开 万艳	讲师 教授 硕士	0134 0134 0134	共振相位调制型光纤SPR传感器理论分析与数值模拟	南京航空航天大学学报	2009.41.06
103	赵志远 曾捷 梁大开 张晓丽	硕士 讲师 教授 博士	0134 0134 0134 0134	一种基于光纤SPR传感器光谱降噪的新方法	光谱学与光谱分析	2009.29.11
104	柳强 陈仁文 明晓	硕士 教授 教授	0134 0134 0121	基于软硬件联合补偿的智能槽道流量计	仪表技术与传感器	2009.12
105	陈仁文 刘强 徐志伟 王鑫伟	教授 博士 教授 教授	0134 0134 0134 0132	基于压电智能结构的垂尾减振系统	力学学报	2009.41.04
106	刘强 王鑫伟 陈仁文 刘琳	博士 教授 教授	0134 0132 0134 外单位	基于灰色预测的自适应解耦控制	南京航空航天大学学报	2009.41.02
107	刘强 陈仁文 刘琳 王鑫伟	博士 教授 教授	0134 0134 外单位 0132	改进的前馈FIR振动控制器	振动与冲击	2009.28.02
108	刘强 陈仁文 王鑫伟	博士 教授 教授	0134 0134 0132	基于正交基函数的广义FIR模型辨识方法	系统工程与电子技术	2009.31.11
109	陈仁文 朱莉娅	教授 博士	0134 0134	大型飞机中的若干关键测控技术及其发展趋势	航空制造技术	2009.08

Front. Mech. Eng. China 2009, 4(2): 153–159
DOI 10.1007/s11465-009-0031-z

RESEARCH ARTICLE

Jinhao QIU, Hao JIANG, Hongli JI, Kongjun ZHU

Comparison between four piezoelectric energy harvesting circuits

Abstract This paper investigates and compares the efficiencies of four different interfaces for vibration-based energy harvesting systems. Among those four circuits, two circuits adopt the synchronous switching technique, in which the circuit is switched synchronously with the vibration. In this study, a simple source-less trigger circuit used to control the synchronized switch is proposed and two interface circuits of energy harvesting systems are designed based on the trigger circuit. To validate the effectiveness of the proposed circuits, an experimental system was established and the power harvested by those circuits from a vibration beam was measured. Experimental results show that the two new circuits can increase the harvested power by factors 2.6 and 7, respectively, without consuming extra power in the circuits.

Keywords energy harvesting, piezoelectric materials, synchronized switching

1 Introduction

The study on piezoelectric energy harvesting has been motivated by the demands on environment monitoring, tunable vibration control, and wireless sensor networks [1–3]. However, the never-ending drive towards self-powered devices poses severe challenges for the energy harvester designer. In particular, raising the efficiency of a piezoelectric energy harvester is becoming increasingly important, especially in the presence of a significant vibration. The existing energy harvesters are simply rectifying the AC output from the piezoelectric elements, and the energy harvesting efficiency is low. However, the efficiency of the piezoelectric energy harvester can be significantly enhanced by using some special electric interface. The first attempt was made by Ottman et al. [4,5]. They developed a circuit that would maximize the power flow from the piezoelectric device; however, several electronic components in the circuit also consumed power. Richard et al. [6–9] proposed a technique called synchronized switch harvesting, which can enhanced the power from piezoelectric elements by 900%.

In this study, a simple source-less trigger circuit used to control the synchronized switch is proposed and two interface circuits of energy harvesting systems are designed based on the trigger circuit. The efficiencies of these two interface circuits are compared with those of the other existing different interfaces.

Received November 18, 2008; accepted December 20, 2008

Jinhao QIU (✉), Hao JIANG, Hongli JI, Kongjun ZHU
The Aeronautic Key Laboratory for Smart Materials and Structures, College of Aerospace Engineering, Nanjing University of Aeronautics and Astronautics, Nanjing 210016, China
E-mail: qiu@nuaa.edu.cn

2 Configuration of piezoelectric energy harvesting system

The piezoelectric energy harvesting system consists of a cantilever beam, piezoelectric element, electromagnet, and rigid base as shown in Fig. 1. The piezoelectric element is bonded at the root of the beam. When the beam is excited by the electromagnet, a large strain is induced on the piezoelectric element, and an AC voltage is generated between the electrodes. The piezoelectric equations of the length expansion are obtained:

$$\begin{cases} D_3 = e_{31}S_1 + \varepsilon_{33}^S E_3, \\ T_1 = c_{11}^E S_1 - e_{31}E_3, \end{cases} \tag{1}$$

where subscripts '1' and '3' refer to the x- and z-direction, respectively.

The x-axis is defined in the length direction, the y-axis is defined in the width direction, and the z-axis is defined in the thickness direction of the beam. The variables E, S, D, and T are the electric field, strain, electric displacement, and stress, respectively. The constants e, ε and c are the

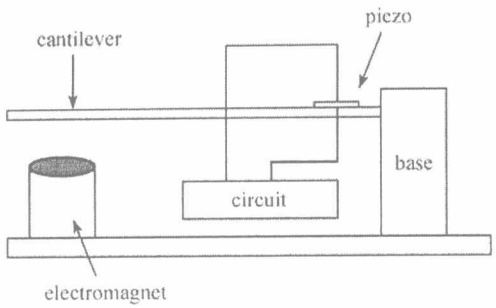

Fig. 1 Configuration of energy harvesting system

piezoelectric constant, dielectric constant, and stiffness. After some manipulations of Eq. (1), the variables E, S, D, and T can be replaced by the voltage V, displacement u, current I, and force F_P, respectively. Using the new variables, Eq. (1) can be rewritten as

$$\begin{cases} I = \alpha \dot{u} - C_0 \dot{V}, \\ F_P = K_{PE} u + \alpha V, \end{cases} \tag{2}$$

where C_0 is the clamped capacitance; α is the force factor; and K_{PE} is the stiffness of the piezoelectric element in a short circuit state.

The following relationships exist between the two sets of variables and constants used in Eqs. (1) and (2):

$$E_3 = -\frac{V}{d}, \tag{3}$$

$$S = \frac{u}{L}, \tag{4}$$

$$I = A_{xy}\dot{D}, \tag{5}$$

$$F_P = A_{yz}T, \tag{6}$$

$$K_P = \frac{c_{31}^E A_{yz}}{L}, \tag{7}$$

$$C_0 = \frac{\varepsilon_{33}^S A_{xy}}{d}, \tag{8}$$

$$\alpha = \frac{e_{31} A_{yz}}{L}, \tag{9}$$

where A and L are the cross-section area and thickness of the piezoelectric, respectively.

3 Four types of interfaces for piezoelectric energy harvesting systems

The power generated by a piezoelectric element cannot be directly used by other electric devices; therefore, some electric interface is necessary for the energy harvesting system to ensure the voltage compatibility with the electric load or energy storage element. There are many different schemes of electric interfaces such as the AC-DC rectifier, voltage doubler, etc.

This section introduces four different types of electronic interfaces that will be used in this study. The most commonly used interface is called the "classic interface", which simply rectifies the AC voltage to DC voltage, while the three other interfaces are developed based on the classic interface.

3.1 Classic interface

The circuit of a piezoelectric energy harvesting system with classic interface is shown in Fig. 2.

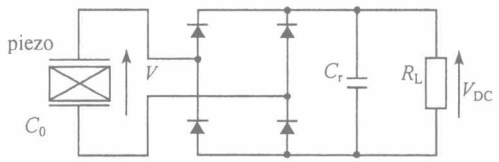

Fig. 2 Classic interface

As shown in Fig. 2, the classic interface includes a diode rectifier and filter capacitor. The terminal electric load is modeled by an equivalent resistor R_L. To calculate the power output of the interface under the condition of single mode vibration, some assumptions should be made. First, the mechanical displacement u is supposed to be purely sinusoidal and the open circuit voltage V on the piezoelectric is also sinusoidal. However, the rectifier is in a blocked state and the piezoelectric element is on an open-circuit state when the absolute value of V is lower than V_{DC}, the voltage across the capacitor. When the absolute value of V is more than V_{DC}, a current I flows through the diodes. The current is divided into two parts, one to the capacitor and the other to the load. The energy E generated in a period T can be estimated by calculating the integration of product of V and I during a period; therefore, the power can be obtained by dividing E by T.

$$P = \frac{4\alpha^2 U^2 \omega^2 R_L}{(2R_L C_0 \omega + \pi)^2}. \tag{10}$$

The power P of the piezoelectric element can also be derived experimentally. When the system is working, by simply measuring the voltage V_{DC} and resistor R_L, the power P can be calculated as:

$$P = \frac{V_{DC}^2}{R_L}. \tag{11}$$

The power for different resistors R_L is not constant, and it is lower when the resistance is very low or very high. There is a maximum power when the resistor has a middle value.

3.2 Voltage doubler interface

The voltage doubler interface is shown in Fig. 3. The Cockroft-Walton voltage doubler circuit can generate high voltages from a low voltage AC source. The circuit is quite practical for some applications when the electric load with a high resistance needs higher power. Using such interface can well optimize the power for different electric loads. For example, if the optimal load for the classic interface is R and the power needs to be maximized at a new resistor of $4R$, then a voltage doubler can be used to match the power and the new resistor. If the resistor changes to $9R$, then a voltage tripler can be employed to optimize the power.

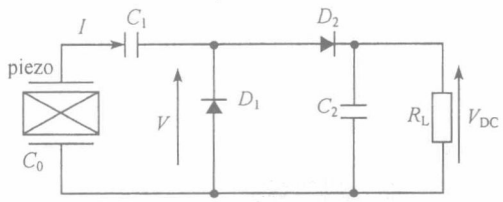

Fig. 3 Voltage doubler interface

The harvested power can be derived either theoretically or experimentally. If the vibration frequency is ω and the tip displacement of the beam is U_M, the DC voltage and output power on the electric load are

$$V_{DC} = \frac{2\alpha U_M \omega R_L}{R_L C_0 \omega + 2\pi\left(1 + \dfrac{C_0}{C_1}\right)}, \tag{12}$$

$$P = \frac{4\alpha^2 U_M^2 \omega^2 R_L}{\left(R_L C_0 \omega + 2\pi\left(1 + \dfrac{C_0}{C_1}\right)\right)^2}. \tag{13}$$

3.3 Synchronous charge extraction interface

The principle of synchronous charge extraction (SCE) is to transfer electric energy accumulated on the capacitor C_0 of the piezoelectric element to the load or energy storage element intermittently. A primary characteristic of this technique is that the intermittent extraction of energy is synchronized with the mechanical vibration. Another peculiarity is that the piezoelectric element is in the open circuit state most of the time.

As shown in Fig. 4, the circuit has a switch S in series with an inductor L that make the charge extraction process work. The switch S is turned off when the voltage V on the piezoelectric element is increasing so that the electric energy is accumulating on the piezoelectric element. Once the voltage V comes to a maximum, the switch S is turned on and the capacitor C_0 of the piezoelectric element is then

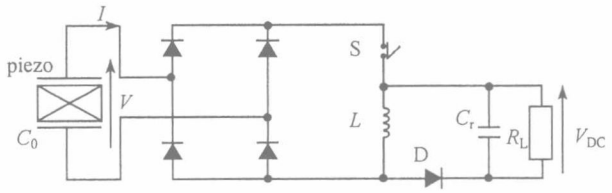

Fig. 4 Synchronous charge extraction interface circuit

discharged through the inductor L. During the discharging process, the high current is induced on the inductor L, and the electric energy is transferred from the capacitor to the inductor. When the charge is completely removed from the capacitor C_0, the switch S is turned off and the piezoelectric is in the open circuit state again. Because the current on the inductor cannot be stopped suddenly, it flows through the branches on the right side. The electric energy on the inductor L is transferred to the capacitor C_r and the electric load R_L due to oscillation effect. The diode D here is used to block the current flow in the inverse direction so that electric charge can be accumulated on the capacitor C_r.

The switching signal and the voltage waveform on the piezoelectric element is shown in Fig. 5. The turned on time of the switch S is very short, approximately 1/50 of the vibration period T.

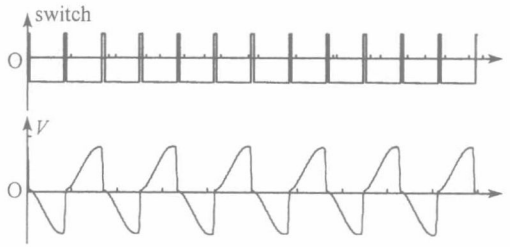

Fig. 5 Switching signal and the voltage waveform on piezoelectric element

The average power can be calculated based on the assumption that the electric energy transferred per period equals the maximal energy accumulated on the capacitor C_0 of the piezoelectric element ideally. Therefore, the expression of the average power delivered by the piezoelectric element is deduced as:

$$P = 2\frac{\alpha^2 U^2 \omega}{\pi C_0}. \tag{14}$$

3.4 Synchronized switch harvesting on inductor interface

The synchronized switch harvesting on the inductor (SSHI) interface utilizes a nonlinear processing circuit connected to the electrodes of the piezoelectric element

and the input side of the rectifier bridge. The nonlinear processing circuit is very simple, consisting of an inductor and a switch, as shown in Fig. 6. The nonlinear processing circuit can increase the voltage amplitude on the capacitor of the piezoelectric element, due to a voltage inversion process. The switch S is turned on when the voltage V on capacitor C_0 of the piezoelectric element reaches a maximum or a minimum. At these triggering instants, an oscillating electrical circuit is established between L and C_0 and the voltage V on C_0 is inversed. The switch S is turned off again after the voltage inversion process is finished. Due to voltage inversion, the voltage V on C_0 increases with time because electric charges are generated by mechanical strains.

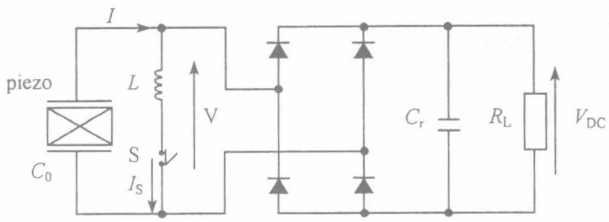

Fig. 6 Synchronized switch harvesting on the inductor circuit

During the voltage inversion process, the absolute value of the voltage V is lower than the voltage V_{DC} on the capacitor C_r so that the current through the rectifier bridge is blocked. The voltage inversion is not perfect so that the absolute value of the voltage after inversion becomes smaller. The voltage inversion loss is mainly due to the equivalent series resistance of the inductor and can be modeled by the electric quality factor Q of the oscillator circuit. Figure 7 shows the illustrative waveforms of the voltages and displacement. The relationship between Q and the voltages of the piezoelectric element before and after the inversion process (V_{DC} and V_m, respectively) is obtained by Eq. (15):

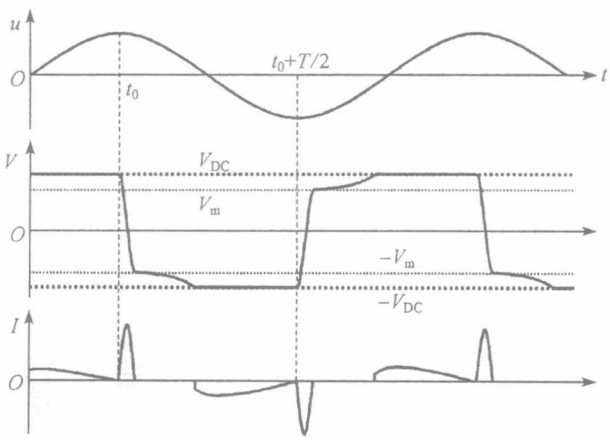

Fig. 7 Voltages and displacement waveforms

$$V_m = -V_{DC}e^{-\pi/2Q}. \tag{15}$$

The electric charge flowing through the equivalent resistance R_L of the terminal load during a mechanical period $T/2$ is balanced by the charged extracted from the piezoelectric element. This leads to

$$-\left(\int_{t_0}^{t_0+T/2} I\mathrm{d}t - \int_{t_0}^{t_0+T/2} I_S\mathrm{d}t\right) = \frac{V_{DC}}{R_L}\frac{T}{2}, \tag{16}$$

where I_S is the current flowing through the inductor. Hence, it is nonzero only during voltage inversion. The first integral is the total charge flowing out of the electrodes of the piezoelectric element and the second integral corresponds to the charge flowing through the inductor during voltage inversion. Hence, the second integral should be the sum of the charge stored on the capacitor C_0 before the voltage inversion and the charge stored on C_0 after the inversion, which is expressed as:

$$\int_{t_0}^{t_0+T/2} I_S\mathrm{d}t = C_0V_{DC}(1+e^{-\pi/2Q}). \tag{17}$$

Substituting Eq. (17) into Eq. (16) and then into the integration of Eq. (2),

$$V_{DC} = \frac{2\omega\alpha U}{R_LC_0\omega(1-e^{-\pi/2Q})+\pi}R_L, \tag{18}$$

where U is the displacement amplitude of mechanical vibration.

The average harvested power P is expressed as

$$P = \frac{V_{DC}^2}{R_L} = \frac{4\alpha^2\omega^2U^2R_L}{(R_LC_0\omega(1-e^{-\pi/2Q})+\pi)^2}. \tag{19}$$

According to Eq. (19), the higher the electric quality factor Q is, the higher the power of the energy harvesting system is. Hence, a high quality and low loss inductor is essential to the circuit.

4 Switch trigger circuit design

The key issue in synchronous charge extraction or synchronized switch harvesting on the inductor is the switch control circuit to turn on and turn off the switch properly. In this section, the two interfaces based on the source-less switch trigger circuit design are introduced.

4.1 SCE Interface

The interface for synchronous charge extraction based on the source-less trigger switch circuit design is shown in Fig. 8. The resistor R, capacitor C, and transistors T_1 and T_2

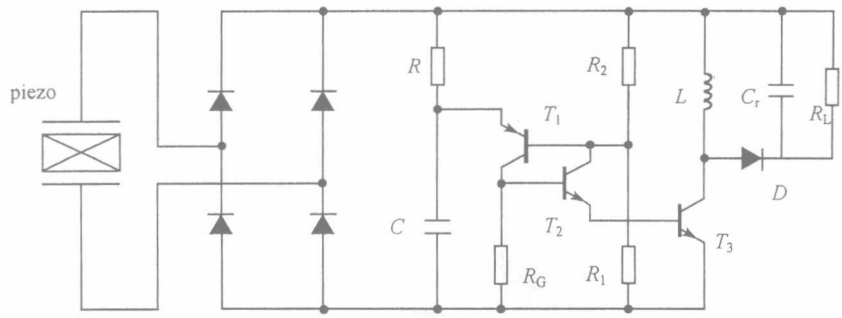

Fig. 8 Solution circuit for synchoronous charge extraction

form the trigger circuit. The transistor T_1 is PNP type, whereas T_2 and T_3 are NPN type. T_1 and T_2 form a programmable unijunction transistor (PUT), which is employed as a trigger and makes the analog switch T_3 turn on and off at the right time. When the voltage V on the piezoelectric element reaches an extremum, the value that the voltage V_A on the emitter of T_1 minus the voltage V_G on the collector T_2 is maximized, and a high level is generated on the emitter of T_2 and the base of T_3. Therefore, the analog switch T_3 is turned on immediately, and the electric energy stored on the piezoelectric element is then transferred into the inductor L. When the electric charge is completely removed from the piezoelectric, the voltage on the base of T_3 changes from high to low, and the analog switch T_3 opens again and the electric energy stored in the inductor L is transferred to the filter capacitor C_r through the diode D. The extraction instants are triggered synchronously with the mechanical vibration. The schematic waveforms on the emitter of T_1 and the collector of T_3 are shown in Fig. 9.

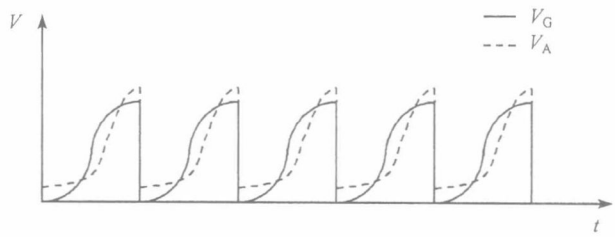

Fig. 9 Voltage waveforms on emitter of T_1 and collector of T_3

4.2 SSHI Interface

The interface for synchronized switch harvesting on the inductor is composed of two sets of switch circuit connected in parallel with the piezoelectric element's electrodes and the input of the rectifier bridge as shown in Fig. 10. Each switch circuit is composed of an inductor L in series with a silicon controlled rectifier (SCR) electronic switch, which is controlled by a switch trigger circuit. When the displacement of the beam is minimum or maximum, one switch trigger circuit is active, while the other one is inactive. The active circuit triggers its switch and an oscillating electric circuit L-C_0 is established. The electrical oscillation period is chosen much smaller than the mechanical vibration period T. The switch will be turned off and the oscillation process is stopped automatically as soon as the current flowing through the *SCR* switch decrease to zero. A similar switching circuit has been proposed by Yabu [10] for semi-active vibration based on SSDI.

One important advantage of the interface circuits presented in this section is that the processing circuits do not need extra power supply. Hence, the harvested energy equals the net output of the energy harvesting system.

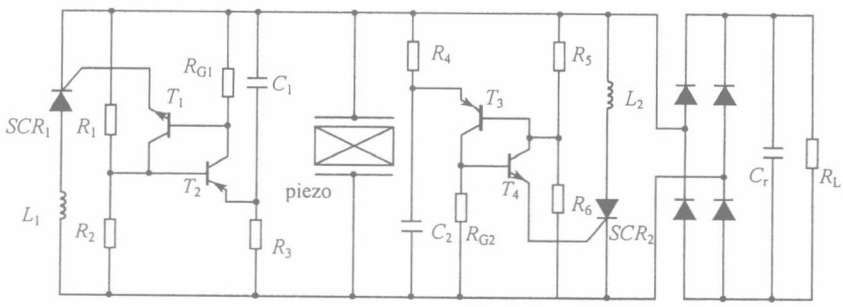

Fig. 10 Solution circuit for synchronized switch harvesting on inductor

5 Experimental results

As shown in Fig. 11, the mechanical part of the experimental setup consists of a steel beam with a dimension of 300 mm×100 mm×2 mm. The piezoelectric element is manufactured by Fuji Ceramics with product number Z0.2T30×30S-SY1-C82, and its dimension is 30 mm×30 mm×0.2 mm. The piezoelectric is attached at the root of the beam, and its electrodes are connected to the electronic interfaces of the energy harvesting system. Four different interfaces are tested in experiment and the power levels of energy harvested from the piezoelectric element are measured. Figure 12 shows the waveforms observed in the experiment of SCE interface based on the energy harvesting system. Figure 13 shows the waveforms observed during the experiment of SSHI interface based on energy harvesting.

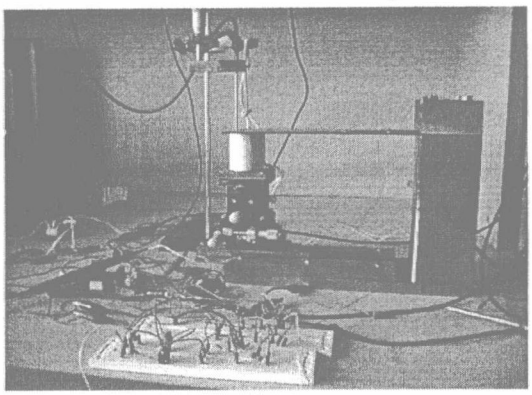

Fig. 11 Experimental setup

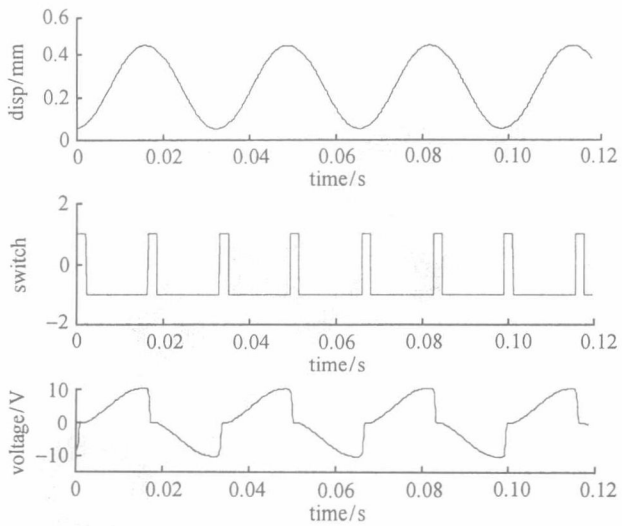

Fig. 12 Measured waveforms of the vibration displacement, switch and voltage on piezoelectric element (SCE interface)

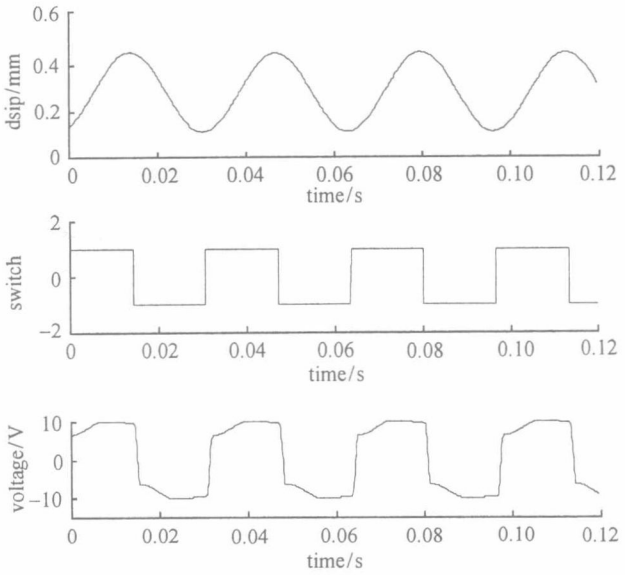

Fig. 13 Measured waveforms of the vibration displacement, switch and voltage on piezoelectric element (SSHI interface)

The theoretical and experimental results of the power of the harvested energy by the four interfaces are shown in Fig. 14. The theoretical values of the power are calculated using the equations presented in Section 3. The first two interfaces are relatively low in efficiency, and the interfaces using synchronized switching technique exhibit much higher efficiency. The SCE interface can enhance the power by 260%, and SSHI interface can enhance the power by 700% compared with the classic interfaces.

The good agreement between the theoretical and experimental results of the energy harvesting system using the SSHI interface means that the designed interface has good efficiency of energy transfer. The experimental power of the SCE interface is much lower than the theoretical value. The difference is partially due to the energy consumed in the switch circuit. Although the energy harvesting circuits do not need the extra power supply, they directly consume power from the piezoelectric element, and the power losses are very low. For SCE interface, the power loss is about 34% of the total generated power, and for SSHI interface, the lower loss is lower than 10% of the total generated power.

6 Conclusions

Four vibration powered piezoelectric energy harvesting interfaces, two of which use the synchronous switching technique, have been investigated and compared. A simple source-less trigger circuit used to control the synchronized switch has been proposed and two interface circuits of energy harvesting systems have been designed based on the trigger circuit. The effectiveness of the proposed

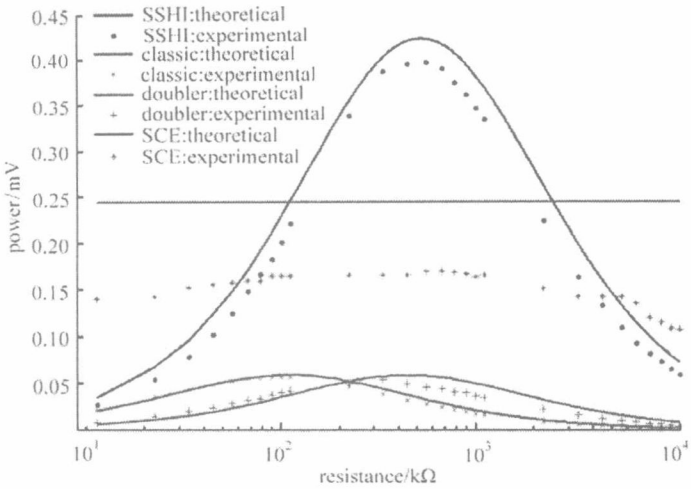

Fig. 14 Theoretical and experimental harvested powers

circuits was validated by the experimental results of energy harvesting systems based on a vibrating beam.

The power levels of the four interfaces are different. According to the experimental results, the synchronized switch harvesting on the inductor interface increases the power of harvested energy by a factor of 7, and the synchronous charge extraction interface has the resistance adaptation capability of the terminal electric load. The synchronized switching technique brings significant improvements to vibration-based piezoelectric energy harvesting systems, thus showing promising possibility of applications in standalone systems and long lifespan intelligent power sources.

Acknowledgements This study was supported by the National Natural Science Foundation of China (Grant No. 50775110).

References

1. Chandrakasan A, Amirtharajah R, Cho S H. Design considerations for distributed microsensor systems. In: Proceedings of the 21st IEEE Annual Custom Integrated Circuits Conference, May16–19, San Diego, 1999: 279–286
2. Davis C, Lssieuter G. An actively tuned solid-state vibration absorber using capacitive shunting of piezoelectric stiffness. Journal of Sound Vibration, 2000, 232: 601–617
3. Rabaey J M, Ammer M J, Julio L. da Silva. PicoRadio supports ad hoc ultra-low power wireless networking. Computer, 2000, 33: 42–48
4. Ottman G K, Bhattt A C, Hofmann H. Adaptive piezoelectric energy harvesting circuit for wireless, remote power supply. IEEE Transactions on Power Electronics, 2002, 17(5): 669–676
5. Hofmann H, Ottman G K, Lesieutre G A. Optimized piezoelectric energy circuit using step-down converter in discontinuous conduction mode. IEEE Transactions on Power Electronics, 2002, 18(2): 696–703
6. Lesieutre G A, Hofmann H, Ottman G K. Damping as a result of piezoelectric energy harvesting. Journal of Sound and Vibration, 2004, 269: 991–1001
7. Guyomar D, Badel A, Lefeuvre E. Toward energy harvesting using active materials and conversion improvement by nonlinear processing. IEEE Transactions on Ultrasonics, Ferroelectrics, and Frequency Control, 2005, 52(4): 584–595
8. Badel A, Benayad A, Lefeuvre E. Single Crystals and nonlinear process for outstanding vibration-powered electrical generators. IEEE Transactions on Ultrasonics, Ferroelectrics, and Frequency Control, 2006, 53 (4): 673–684
9. Lefeuvre E, Adrien B, Claude R. A comparison between several vibration-powered piezoelectric generators for standalone systems. Sensors and Actuators A, 2006, 126: 405–4
10. Yabu T, Onoda J. Non-power-supply semi-active vibration suppression with piezoelectric actuator. In: Proceedings of the 47th Symposium on Structural Strength, Japan Society of Astronautics, Kanazawa, Japan, July 20-22, 2005: 48–50

Energy Harvesting and Vibration Control Using Piezoelectric Elements and a Nonlinear Approach

J.H. Qiu, H.L. Ji and H. Shen
Aeronautic Science Key Laboratory for Smart Materials and Structures,
Nanjing University of Aeronautics and Astronautics,
#29 Yudao Street, Nanjing 210016, China
qiu@nuaa.edu.cn

Abstract —The piezoelectric materials, as the most widely used functional materials in smart structures, have many outstanding advantages for sensors and actuators, especially in vibration control and energy harvesting, because of their excellent mechanical-electrical coupling characteristics and frequency response characteristics. Semi-active vibration control based on state switching and pulse switching, have been receiving much attention over the past decade because of several advantages. The technique is based on a nonlinear processing of the voltage delivered by the piezoelectric elements. This process increases the amount of electrically converted energy during a mechanical loading cycle of the piezoelectric element. A new approach for energy harvesting from mechanical vibrations is also derived from the nonlinear approach based on Synchronized Switch Damping. The present research activities of vibration control and energy harvesting using piezoelectric elements and a nonlinear approach are introduced.

INTRODUCTION

Since conventional passive damping materials have reached their limits to damp vibration because it is not very effective at low frequencies and requires more space and weight, new control designs with novel actuator systems have been proposed. These so called smart materials can control and suppress vibration in an efficient and intelligent way without causing much additional weight or cost. The vast majority of research in smart damping materials has concentrated on the control of structures made from composite materials with embedded or bonded piezoelectric transducers because of their excellent mechanical-electrical coupling characteristics.

A piezoelectric material responds to mechanical force by generating an electric charge or voltage. This phenomenon is called the direct piezoelectric effect. On the other hand, when an electric field is applied to the material mechanical stress or strain is induced; this phenomenon is called the converse piezoelectric effect. Due to their excellent electromechanical coupling characteristic, piezoelectric materials have widely been used in structural vibration control, structural health monitoring, and energy harvesting. The direct effect, the function of mechanical-to-electrical energy conversion, is used for sensing, energy harvesting or vibration damping and the converse effect, the function of electrical-to-mechanical energy conversion, is for actuation.

Vibration in modern structures like airplanes, satellites or cars can cause malfunctions, fatigue damages or radiate unwanted and loud noise [1-6]. Vibration control using piezoelectric materials has been one of the most important research fields in smart structures. The methods of vibration control using piezoelectric transducers can be mainly divided into three categories: passive, active, and semi-active. In different vibration control systems, the piezoelectric transducers play different roles. In a passive control system, usually the *R-L* shunt circuit is used to consume the electrical energy converted from mechanical energy by the piezoelectric transducer [7-8], and consequently reduce the mechanical vibration. In a semi-active control system, the voltage on the piezoelectric transducer is processed nonlinearly by switched shunt circuit to increase its magnitude and change its phase so that the mechanical- to-electrical energy conversion is maximized. In an active vibration system, a control command is applied to the piezoelectric transducer. In summary, piezoelectric transducers are used for electrical-to-mechanical energy conversion in passive and semi-active vibration control systems, but they are used for electrical-to-mechanical energy conversion in active control systems. The passive methods are simplest among the three categories, but their control performance is sensitive to the variations of the system parameters. Moreover, the passive control systems usually need large inductance in low frequency domain, which is difficult to realize. Active control systems require high-performance digital signal processors and bulky power amplifiers to drive actuators, which are not suitable for many practical applications. Semi-active methods can overcome the drawbacks of both passive and active methods, but more sophisticated switch control methods need to be developed for their application in multimode vibration control.

Vibration energy harvesting has also attracted much attention because of its potential application in power supplies for low-power electronic devices, such as structural health monitoring systems, wireless devices and semi-active vibration control systems. In an energy harvesting system, the electrical energy converted from mechanical energy by the piezoelectric transducer is collected by an electronic circuit and stored in a capacitor or battery. The similar techniques for semi-active vibration control system have been used to boost the efficiency of energy harvesting systems.

PRINCIPLE OF ENERGY CONVERSION IN PIEZOELECTRIC TRANSDUCERS

978-1-4244-4970-5/09/$25.00 ©2009 IEEE